Journal of Civil Engineering and Urban Planning (2024)
Clausius Scientific Press, Canada

DOI: 10.23977/jceup.2024.060224
ISSN 2616-3969 Vol. 6 Num. 2

Study on the Nondestructive Detection Method of Tunnel Lining Crack and Empty Ring Disease

Gaowen Wu*

Tieeighth Bureau Group Third Engineering Co., LTD, Guiyang, Guizhou, 520100, China
553102056@qq.com
**Corresponding author*

Keywords: Tunnel, Lining, Non-Destructive Testing, Geological Radar, Inversion Analysis

Abstract: In order to detect the width, depth of the tunnel lining crack and the depth and range of the empty ring, and analyze the tunnel lining strength in the disease area to ensure the quality of the project. Firstly, ultrasonic and geological radar are used for scanning, and the scanning image is analyzed, so as to determine the width, depth, depth and range of the tunnel lining crack. Finally, the test results show that the ultrasonic and geological radar inversion analysis of the width and the depth of the tunnel lining crack first group are 3.14mm and 91.1mm respectively, the second group is 3.17mm, 75.8mm respectively, the length of the first group of core sampling is 90.0mm, the second group is 75mm, the error rate is 1.05%~1.2%, high confidence. The minimum strength of point load test concrete is 44.32 MPa, the maximum value is 53.48583 MPa, and the average value is 48.4 MPa, which meets the requirements of lining strength C35 concrete.

1. Preface

According to statistics, by the end of 2020, China's railway operating mileage had reached 145,000 km, among which 16,798 railway tunnels were put into operation, with a total length of about 19,630 km. Due to the complex geological conditions and rich groundwater in the karst area of Guizhou, cracking and water seepage often occur during the operation period of high-speed railway tunnel, which seriously threatens the operation safety of high-speed railway.

Nondestructive detection has the advantages of fast, high efficiency and strong anti-interference ability, and the resolution ability can reach centimeter level. In terms of tunnel detection, automatic rapid nondestructive testing technology is an important direction of tunnel detection development, especially in image automatic recognition, vehicle detection radar, micro seismic monitoring technology of rapid detection technology, in the tunnel bad geology, steel arch anchor spray joint support and cavity disease detection application more and more widely. In recent years, especially radar and ultrasonic nondestructive testing technology has been more and more widely studied and applied in the field of railway tunnel and highway tunnel lining quality testing [1-3].

2. Nondestructive Testing Technology Theory

2.1 Ultrasonic Detection Theory

The physical and mechanical properties of concrete are restricted by many factors, such as its internal structural characteristics and external environmental conditions, and its acoustic wave propagation characteristics reflect the stress and strain relationship of concrete. According to the wave theory in elastic-plastic medium, the velocity of stress wave is:

$$V_P = \sqrt{\frac{E(1-\mu)}{\rho(1+\mu)(1+2\mu)}} \tag{1}$$

Where E is the dynamic elastic modulus of the medium, ρ is the density, and μ is the Poissant ratio. While there is a correlation between the elastic modulus and the strength of the medium. The correlation between the propagation parameters of ultrasonic wave in concrete (sound value, sound value, sound velocity, wave amplitude, attenuation coefficient, etc.) and the physical and mechanical indexes of concrete medium (moving mode, density, strength) of concrete medium is the theoretical basis of ultrasonic detection. When the internal and external factors such as material, uniformity and construction conditions of the concrete medium are basically consistent, the propagation parameters of the ultrasonic wave should be basically the same, the ultrasonic wave produces diffraction, reflection and attenuation in the propagation process, causing the sound time, sound velocity and frequency spectrum. High precision acoustic reflection — receiving instruments and sensors can record and describe the intrinsic quality of concrete.

2.2 Radar Detection Principle

The detection principle of geological radar (Ground Penetrating Radar, GPR) is a broad spectrum (1 MHz to 1GHz) electromagnetic technology used to determine the distribution of underground media. It can be widely used in shallow concrete structure, structure and shallow geological structure, structure and lithology detection. It is a geophysical exploration method that uses the ultra-high frequency pulse electromagnetic wave as the source and in the form of self-excitation, and can detect the distribution of underground medium in the form of continuous and intermittent. It has the characteristics of fast, non-destructive, continuous detection and real-time display.

The detection principle of geological radar is determined according to the propagation law of the ultra-high frequency short pulse (10^6-10^9Hz) electromagnetic wave in the structural medium.

When the electromagnetic wave travels in the medium, its path, the strength of the electromagnetic field, and the waveform will change with the electrical properties and geometry of the passing medium. Therefore, the structure of the medium can be inferred based on the travel time of the received wave, amplitude and waveform data [4-6].

Because the distance between the transmitting antenna of the geological radar and the receiving antenna is very small, it even merges into one. When the inclination of the detected structure is not large, the entire path of the reflected wave is almost vertical plane. Therefore, the change of the normal reflection time at different positions of the measuring line reflects the structural morphology of the inspected structure. Geological radar working frequency is high, and the displacement current is mainly used in the engineering and geological medium. Therefore, the high frequency broadband band electromagnetic wave propagation, essentially very little scattered, the speed is basically determined by the dielectric properties of the medium. Therefore, the theory of electromagnetic wave propagation and the theory of elastic wave propagation have many similarities. Both follow the same form of the wave equation, but the physical meaning of the variables in the wave equation

is different. The theory of geological radar detection is based on the geological radar following the same form of wave equation, but the physical significance of the variables in the wave equation is different. The theory of geological radar detection is based on the dielectric constant of geological radar, and the detection effect of radar detection mainly depends on the electrical difference of different media interfaces, that is, the greater the difference between the dielectric layers, the better the detection effect, and the more obvious the medium anomaly is reflected in the radar profile, so that it is easy to identify. During the actual measurement, the radar wave enters the lining and surrounding rock through the antenna. When the medium with different material is encountered, the interface reflection is generated. When the receiving antenna receives the reflected wave and measures the reflected wave $t = \frac{\sqrt{4z^2 + x^2}}{v}$, the distance of the reflected wave can be calculated, so as to find the distance between the antenna and the reflected surface $z = \frac{v \times t}{2}$ (Figure 1). Where z is the distance from the antenna to the reflecting surface (m); t is the radar wave with ns (nanosecond), 1ns=10^{-9} seconds; x is the inter-antenna distance (m); v is the walking speed (m / ns); and the transmission and reflection of straight transmitted radar waves can be viewed with the concept of geometric optics. Where C0 is the propagation speed of radar wave in air about 30cm / ns; ε is the dielectric constant, which is determined by the matter through which the wave.

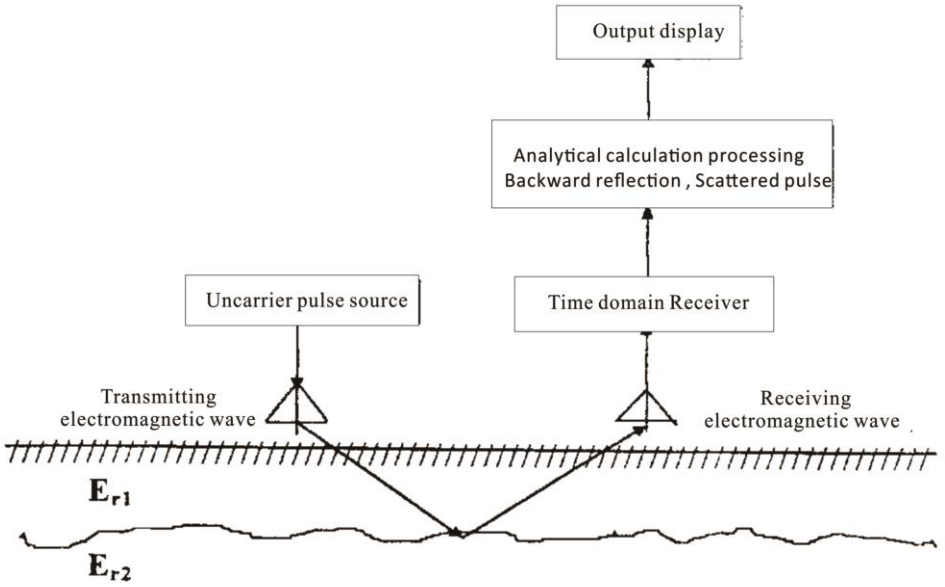

Figure 1: Schematic diagram of the radar detection principle

3. NDT and Analysis of High-Speed Railway Tunnel

3.1 Project Overview

Niuchangpo Tunnel is located in Xifeng County, the eastern edge of Guizhou. The elevation of the area is 1120~1170m, and the relative elevation is 50m, which is a low Zhongshan landform. The maximum buried depth of the tunnel is 37m. The area belongs to the middle subtropical plateau monsoon humid climate, abundant rainfall, divided into dry and wet two seasons. The tunnel site of the mountain is steep, and the surface runoff conditions are good. The atmospheric rainfall mostly flows into the ditch along the slope, and the surface is poor, mainly seasonal water flow. Tunnel site

groundwater mainly karst water, the atmospheric precipitation supply water, due to the slope runoff condition is good, the atmospheric rainfall part along the slope drainage, partial dissolution surface cracks, did not see the groundwater exposure, under the Permian group with gray, light gray thick layered limestone is given priority to, change strata strong and rich water, karst strong development. The design surrounding rock level of tunnel area is mainly IV and V. The tunnel adopts composite lining, the initial support is anchor rod, advance small pipe, wet spray concrete, I-steel arch, steel grille arch as the main means, and the secondary lining adopts reinforced concrete and plain concrete [7-8].

3.2 Test Method and Conclusion

In order to study the crack width and depth, ultrasonic wave is used to detect the crack depth and width. The ZBL-F103 type crack width detector produced by Beijing Zhibo Lian Company was tested, as shown in Figure 2. The measurement range is 0 to 6 mm and the measurement accuracy is ±0.01mm.

Figure 2: ZBL-F610 type crack depth gauge

The test results are as follows (as shown in Table 1 and Figure 3):

Table 1: Detection of arch roof concrete cracks

ID	Tunnel name	Detection of crack in arch roof concrete			
		No.	Width mm	Depth mm	Judge
S11	New street 2 # tunnel	1	3.14	91.1	
		2	3.17	75.8	

Figure 3: Field photos of ultrasonic detection of cattle farm slope tunnel

In order to study the location and range of tunnel lining, radar NDis test, and the radar test parameters are as follows:

Sampling frequency: 25,000 MHz

Number of sampling points: 8,192 points
Add number: automatic addition
Window time: 50 (ns)
Lane spacing: 0.01 (m)
Reference wave speed: 0.1m / ns
Working mode: continuous mode

Due to the different depth range of antennas at different frequencies, the higher the frequency, the smaller the detection depth, and the clearer the results of the detection images. The antenna frequency of this detection is 900 MHz. This time mainly tests the defects behind the lining, and then evaluates the quality according to the specification requirements. The instruments used are as follows:

(1) Beijing High-speed Railway Construction Department concrete crack comprehensive detector (instrument number: GTJ-F800).

(2) RadarVIEW1 acquisition software and GprView20190104OLD data analysis software.

The test results are shown in Figure 4.

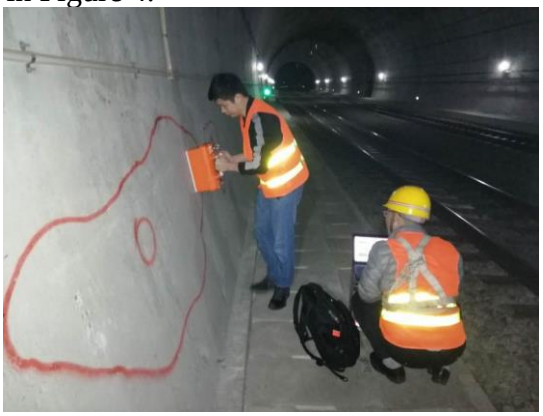

Figure 4: Geological radar detects the defects of side wall lining

4. Drilling and Coring On-Site Verification

In order to verify the reliability of ultrasonic and geological radar nondestructive testing results (in Figure 5 and Figure 6), on-site drilling and coring were carried out.

Figure 5: Measurement of the crack depth of the first set of drilling core sampling

Figure 6: Crack depth measurement of the second set of drill core sampling

The length of the first group is 90.0 mm and the second group is 75 mm. According to the width and depth of tunnel lining cracks according to ultrasonic and geological radar inversion, the first group is 91.1 mm, 3.14 mm and the second group is 3.17 mm, 75.8 mm respectively. Through the comparative analysis of field sampling, the error rate is 1.05%~1.2%, with high confidence.

5. Test and Analysis of the Tunnel Lining Quality in the Disease Area

Because the concrete test in the disease area needs to test the concrete test block, so the point load test is used to test and calculate the concrete strength (in Table 2). The test method is as follows:

(1) Uncorrected rock point load strength is calculated in the following formula:

$$I_s = \frac{P}{D_e^2} \tag{2}$$

Where: I_s- -uncorrected rock point load strength (MPa);

P- -Damage load (N);

D_e- -Equivalent core diameter (mm).

(2) The equivalent core diameter is calculated by radial test according to the following formula:

$$D_e^2 = D^2 \tag{3}$$

$$D_e^2 = DD' \tag{4}$$

Where: D- -loading point spacing (mm);

D' - -Loading point spacing (mm) after the failure of the upper and lower cone ends.

(3) The equivalent core diameter of axial, block or irregular block test is calculated according to the following formula:

$$D_e^2 = \frac{4WD}{\pi} \tag{5}$$

$$D_e^2 = \frac{4WD'}{\pi} \tag{6}$$

Where: W- -the width or average width (mm) through the minimum section of the two loading points.

Where: W- -the width or average width (mm) through the minimum section of the two loading

points.

(4) If the equivalent core diameter is not equal to 50mm. When the test data is large and the equivalent core diameter in the same group of specimens has multiple sizes but not equal to 50mm, according to the test results (in Figure 7), the relationship curve between D_e^2 and failure load P is drawn, and the corresponding P50 value when D_e^2 is 2500mm^2 is found on the curve, and the rock point load strength index is calculated in the following formula:

$$I_{s\ (50)} = \frac{P_{50}}{2500} \tag{7}$$

Where: $I_{s\ (50)}$ - - -Rock point load strength index (MPa) with an equivalent core diameter of 50mm;

P_{50}- -P value (N) of D_e^2 at 2500mm^2 obtained from theD_e^2 ~P relationship curve.

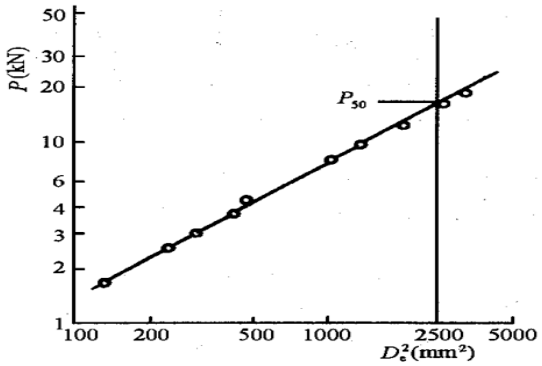

Figure 7: The log relation curve of $P \sim D_e^2$

(5) When the diameter of the equivalent core is not 50mm and the test data is small, it should not be corrected according to the above (4) method, and the rock point load strength index is calculated according to the following formula:

$$I_{s\ (50)} = FI_s \tag{8}$$

$$F = \left(\frac{D_e}{50}\right)^m \tag{9}$$

Where: F- -correction coefficient;

The m- -correction index, 0.40~0.45, or according to the empirical value of similar rocks.

(6) The anisotropy index of rock point load strength is calculated by following the following formula:

$$I_{a\ (50)} = \frac{I'_{s\ (50)}}{I''_{s\ (50)}} \tag{10}$$

Where: $I_{a\ (50)}$ --Anisotropic index of rock point load strength;

$I'_{s(50)}$ --Rock point load strength index perpendicular to the weak surface(MPa);

$I''_{s(50)}$ --Point load strength index (MPa) parallel to the weak surface(MPa).

(7) The point load strength index of vertical and parallel weak surface rock calculated by formula (8.6) is averaged. When a set of valid test data does not exceed 10, discard the highest and lowest values, then calculate the average of the remaining data; when a set of valid test data exceeds 10, discard 2 highest values and 2 lowest values in turn, and then calculate the average value of the remaining data.

(8) Take the calculated value of 3 valid digits.

(9) Test records of rock point load strength include project name, sampling location, specimen number, specimen description, water content status, test type, specimen size and damage load.

Table 2: Point load test record of vault concrete sample

Instrument name and serial number		Rock point load tester (digital) number: 1440				
The specimen number		No.1 sample	No.3sample	No.4sample	No.5 sample	No.6 sample
Sampling depth						
Sample shape		quasi-cylinder	quasi-cylinder	quasi-cylinder	quasi-cylinder	quasi-cylinder
colour		ash black	ash black	ash black	ash black	ash black
mineral composition		concrete	concrete	concrete	concrete	concrete
Water content status (moisture content%)		native state	native state	native state	native state	native state
sample size	Diameter (mm)	43.14	43.04	43.14	42.96	43.36
	Defect edge (mm)	33.46	36.88			39.00
	Mean thickness (mm)	26.16	17.42	21.36	15.88	50.46
Direction of loading		Axial loading	Axial loading	Axial loading	Axial loading	Radial loading
Destruction Loading P(kN)		2.94	2.59	3.59	1.65	4.27
Distance between loading points D(mm)		24.84	2.59	23.14	11.64	42.00
Disage face minimum width b_{f1}		12.66	15.82	21		15.94
Maximum width of the destruction surface b_{f2}		24.24	25.1	23.74		32
Width of the destruction surface W_f(mm)		36.9	40.92	44.74	42.08	37.6329
Width of the destruction surface		1167.046	943.0274	1318.164	623.647	2012.459286

D_e^2(mm^2)					
Uncorrected point load strength I_s(MPa)	2.51918	2.746474	2.723485	2.645727	2.121782056
coefficient of correction F	0.850538	0.812876	0.872833	0.744496	0.954948075
Revised point load strength index $I_{s\ (50)}$ (MPa)	2.14266	2.232542	2.377148	1.969733	2.026191689
Revised point load strength index R_c(MPa)	48.20984	50.23219	53.48583	44.31899	45.589313

Note: 1) The test shall be carried out in strict accordance with the Standard of Test Method for Engineering Rock Mass (GBT50266-2013).

2) According to the recommended method of the International Committee for Rock mechanics Test Methods (revised in 1985) Rc = (20-25) $I_{s\ (50)}$, this test) Rc = 22.5 * $I_{s\ (50)}$.

6. Conclusion

Through ultrasonic and radar scanning techniques, the width, depth and range of crack in the slope tunnel were analyzed. The first group is 91.1 mm, 3.14 mm, and the second group is 3.17 mm, 75.8 mm, and the length of the second group is 75 mm, with the error rate of 1.05%~1.2%, with high confidence.

Then, the point load test is used to analyze whether the tunnel quality in the disease area is healthy and calculated. The minimum strength of the test concrete is 44.32 MPa, the maximum value is 53.48583 MPa, and the average value is 48.4 MPa, which meets the requirements of lining strength C35 concrete.

References

[1] Ye Liangying. Research on radar detection of subway tunnel lining [D]. Shantou University, 2005.

[2] Wang Dongdong, Wei Chenbing. Study on the lining crack disease and its control measures of high-speed railway tunnel [J]. Mingcheng Painting, 2020.

[3] Ma Huaichao. Study on the lining crack disease and its control measures of high-speed railway tunnel [J]. China's Science and Technology, 2020.

[4] Qin Chengke. Research on the detection technology of tunnel lining diseases based on numerical analysis [J]. Western Transportation Technology, 2020, (5): 5.

[5] Yang Guang, Chen Tianjiao, Li Pan, et al. Application of ultrasonic and radar method in crack detection of tunnel lining [J]. Hunan Transportation Technology, 2020, 46 (1): 4.

[6] Guan Pu. Model on the evolution of thin-wall hole defects in high-line tunnel vault [D]. Beijing University of Civil Engineering and Architecture, 2020.

[7] Zan Wenbo, Zhao Chunchen, Wang Ning, Yang Qian. Review of tunnel detection and health status evaluation studies [J]. Mechanization, 2020, 37 (10): 8.

[8] Tang Chao, Liu Chun, Zhou Zeqi. Analysis of research status of operating tunnel lining diseases [J]. Modern Salt Chemical Industry, 2021 (2): 109-110.